Intrastream variability in solute transport: Hydrologic and geomorphic controls on solute retention

Sopan Patil,[1,6] Timothy P. Covino,[2] Aaron I. Packman,[3] Brian L. McGlynn,[2] Jennifer D. Drummond,[3] Robert A. Payn,[4] and Rina Schumer[5]

[1]   Hydrologic fluctuations and geomorphic heterogeneity are expected to produce substantial variability in solute transport within rivers. However, this variability has not been sufficiently explored due to the limited availability of solute injection data in most rivers. Here, we analyzed 81 tracer injection breakthrough curves (BTCs) along Stringer Creek, a 5.5 km^2 watershed in Montana. BTC measurements were obtained for three baseflow conditions at 27 reaches along a 2600 m stream channel. BTCs in upstream reaches (first 1400 m) had receding tails with shallow slopes, indicating high solute retention. Conversely, BTCs in downstream reaches (1400 to 2600 m) had receding tails with steeper slopes, indicating low solute retention relative to upstream reaches. Difference in BTC tails along the stream channel coincided with changes in channel morphology and bedrock geology. Specifically, channel slope increases from 5–6% (upstream) to 9% (downstream), channel sinuosity decreases from a maximum of 1.32 (upstream) to 1.02 (downstream), and the underlying bedrock changes from sandstone (upstream) to granite-gneiss (downstream). Importantly, intrastream differences in BTC tails were distinctly observable only during the two lowest baseflow conditions. Spatial variability of BTC tail-slopes was most sensitive to changes in local discharge at low flow, and to changes in channel sinuosity at high flow. BTC tail-slopes varied temporally with local discharge and velocity at upstream reaches, but not at downstream reaches. These results suggest that local interactions between channel morphology and solute retention vary with hydrologic conditions, and that solute retention becomes more homogeneous at higher stream discharge.

Citation: Patil, S., T. P. Covino, A. I. Packman, B. L. McGlynn, J. D. Drummond, R. A. Payn, and R. Schumer (2013), Intrastream variability in solute transport: Hydrologic and geomorphic controls on solute retention, *J. Geophys. Res. Earth Surf.*, *118*, 413–422, doi:10.1029/2012JF002455.

1. Introduction

[2]   Solute transport in rivers is a complex process due to the heterogeneity in geomorphic and hydrologic properties of stream channels. Solute transport into in-stream dead-zones and subsurface hyporheic flow paths significantly increases the time scale of solute retention [*Bencala*, 2006; *Gooseff et al.*, 2008]. Studies of individual stream reaches have shown that solute retention depends on numerous factors, including stream discharge [*Zarnetske et al.*, 2007], channel bedrock geology [*Harvey and Wagner*, 2000], physical size of the hyporheic zone [*Tonina and Buffington*, 2009], and presence of structural features like bedforms and meanders [*Wörman et al.*, 2002; *Cardenas et al.*, 2004; *Boano et al.*, 2006]. These factors play an important role in structuring the stream and subsurface ecosystems [*Jones and Mulholland*, 2000], influence the migration of fine suspended particulate matter through rivers [*Packman et al.*, 2000a, 2000b; *Packman and MacKay*, 2003; *Karwan and Saiers*, 2009], and control the opportunity for microbial processing of carbon and nutrients [*Battin et al.*, 2008; *von Schiller et al.*, 2008; *Alexander et al.*, 2009]. However, it is not fully understood how solute retention in rivers is influenced by the spatial and temporal variability in hydrology, morphology, and hydrogeology. This influence needs to be better understood to address a variety of engineering and management applications, such as contaminant removal [*Choi et al.*, 2000; *Hussein and Schwartz*, 2003], management of mine tailings [*Boult et al.*, 1994; *Da Silva et al.*, 2005], and stream restoration [*Bockelmann et al.*, 2004; *Bukaveckas*, 2007; *Hester and Gooseff*, 2010; *Doyle and Fuller*, 2011].

[1]School of Civil and Environmental Engineering, Georgia Institute of Technology, Atlanta, Georgia, USA.
[2]Nicholas School of the Environment, Duke University, Durham, North Carolina, USA.
[3]Department of Civil and Environmental Engineering, Northwestern University, Evanston, Illinois, USA.
[4]Department of Land Resources and Environmental Sciences, Montana State University, Bozeman, Montana, USA.
[5]Division of Hydrologic Sciences, Desert Research Institute, Reno, Nevada, USA.
[6]Now at National Health and Environmental Effects Research Laboratory, U.S. Environmental Protection Agency, Corvallis, Oregon, USA.

Corresponding author: S. Patil, National Health and Environmental Effects Research Laboratory, U.S. Environmental Protection Agency, Corvallis, OR 97333, USA. (sopan.patil@gmail.com)

[3] Numerous reach-scale tracer injection studies have provided important insights into the potential causes of stream solute retention. *Harvey et al.* [1996] measured the concentrations of a tracer injected at an experimental river reach in Colorado and found that the surface-subsurface exchange of stream water was dependent on flow conditions. The authors showed that greater exchange and solute retention occurred at low-flow conditions, whereas the surface-subsurface exchange decreased by 30% when the baseflow increased 10-fold. *Wondzell* [2006] conducted stream tracer experiments in steep mountain streams in western Oregon and observed that the presence of physical barriers in channels, such as log-jams, increased the transient storage of stream water and associated solutes. However, as this storage was primarily induced by elevation head gradients, it was relatively insensitive to changes in streamflow. *Salehin et al.* [2003] analyzed multiple solute injection breakthrough curves (BTCs) in an agricultural stream reach in Sweden and found that farming practices such as channel excavation increased solute residence times and decreased the effective hyporheic exchange rate. *Gooseff et al.* [2007] hypothesized that transient storage increases with channel geomorphic complexity, and further that the geomorphic complexity decreases with human modifications. Using tracer injections of Rhodamine WT, they noted that residence times and transient storage were greater in natural stream reaches with native vegetation than in anthropogenically modified reaches. More detailed analyses have confirmed the importance of channel morphology to hyporheic exchange and solute storage. Using an explicit multiscale model, *Stonedahl et al.* [2010] showed that the spatial variability in both hyporheic exchange and transient storage times increases dramatically with channel complexity. While such studies have greatly improved our understanding of the mechanisms governing solute retention, this reach-based knowledge tends to be piecemeal, and therefore, we still have an incomplete understanding of how solute retention is organized across larger scales.

[4] Transient storage models (TSM) [*Bencala and Walters*, 1983; *Runkel*, 1998; *Wörman et al.*, 2002] are commonly used to assess solute retention and transport from tracer injection results. The TSM is often fit to measured BTCs in an attempt to identify reach-scale effective transport properties such as the size of transient storage reservoir, the rate of surface-subsurface exchange, and the characteristic timescale of solute storage. However, several studies have suggested that the difficulty in relating TSM parameters to channel conditions is a major obstacle to generalizing site-specific findings [*D'Angelo et al.*, 1993; *O'Connor et al.*, 2010; *Szeftel et al.*, 2011]. *Zarnetske et al.* [2007] analyzed the TSM parameters on five diverse streams in Arctic Tundra and found that the mean storage residence time showed an exponential decline with increase in stream discharge, but no clear relationship with the extent of the hyporheic zone (permafrost active layer depth). *Wondzell* [2006] found that the parameters from TSM did not conform to the direct observations of solute retention and noted that the model parameters have low sensitivity to longer residence time flow paths and high sensitivity to changes in discharge. *Szeftel et al.* [2011] suggested that tracer BTCs lack sufficient

information to identify a single, unique TSM parameter set. Very recently, *Stonedahl et al.* [2012] demonstrated that tracer storage inferred from TSM fits does not reflect the breadth of hyporheic transport timescales, even in relatively simple and constrained streams. Our ability to generalize findings from individual stream reaches is further hampered by the limited availability of high-quality solute injection data [*Drummond et al.*, 2012]. As a result, the spatiotemporal variability in solute retention within river systems remains poorly characterized.

[5] In spite of the difficulties mentioned above, important solute transport characteristics can be inferred from BTCs since they describe the distribution of solute travel times to a given point downstream of a tracer injection. The peak of the curve represents the effects of mean in-stream advection, while the width of the peak reflects the distribution of in-stream velocities (dispersion). Skewness and long receding tails reflect the impact of solute storage, as the solute is effectively immobilized from the main channel and re-released at a later time [*Schumer et al.*, 2003]. Receding tails with shallow slopes correspond to longer solute retention, whereas steep BTC tail slopes indicate short-term solute retention and faster overall transport through the stream reach [*Haggerty et al.*, 2002; *Salehin et al.*, 2003]. In this study, our focus is only on the distribution of solute residence time in storage zones, and therefore, we limit our analysis to the characteristics of the receding tails of measured BTCs. For a more complete description of the distinction between in-stream advection, dispersion, and storage, see *Schumer et al.* [2009] and *Boano et al.* [2007].

[6] Here we investigate the extent to which hydrologic and geomorphic properties control spatiotemporal variability in solute retention along a stream. We analyze a published dataset of 81 salt-injection BTCs measured in the stream channel of Stringer Creek, a $5.5\,km^2$ mountainous headwater watershed in Montana [*Payn et al.*, 2009, 2012]. Our study was performed as part of a larger synthesis of stream solute studies encompassing 162 tracer injections in 87 streams [*Drummond et al.*, 2012]. The dataset analyzed here is unique in that it contains results from a series of tracer injections that were repeated not only over a long stream valley (2600 m) spanning two distinct underlying geologies, but also through changing discharge conditions. We compare receding tails of solute BTCs measured in 27 reaches along the stream and at three different flow conditions spanning a summer baseflow recession. We then assess the variability in solute retention associated with changes in channel morphology along the stream, as well as changes in stream flow over time.

2. Data and Methods

2.1. Study Site

[7] The tracer injection experiments were performed during the summer baseflow recession in 2006 along the stream channel of Stringer Creek, a $5.5\,km^2$ watershed located within Tenderfoot Creek Experimental Forest (TCEF) in Montana, United States (Figure 1). TCEF is located in the Little Belt Range of the Rocky Mountains and is managed by the United States Department of Agriculture Forest Service. Tracer experiments were conducted along a 2600 m stream segment
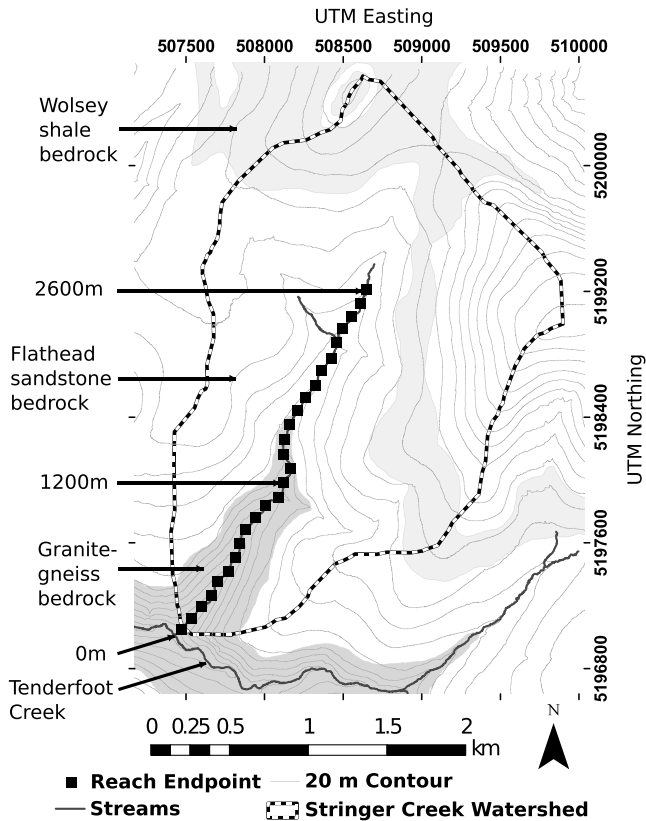
Figure 1. Map of Stringer Creek (latitude 46°55′N, longitude 110°52′W) illustrating the watershed boundary, lithologic features, stream channel, and the BTC measurement locations (adapted from *Payn et al.* [2009]).

Figure 2. Channel sinuosity and channel bed slope at the 27 small reaches along the Stringer Creek channel. Black dash-dot line indicates the lithologic transition that divides the upstream and downstream reaches.

of Stringer Creek, starting near its confluence with Tenderfoot Creek, progressing upstream, and ending near the origination of perennial flow. A perennial stream flows into the Stringer Creek main channel about 2200 m upstream from its confluence with Tenderfoot Creek (Figure 1).

[8] Stringer Creek channel structure changes abruptly at approximately 1200 m upstream from the watershed outlet. This transition corresponds to the change in valley-floor bedrock from sandstone (upstream) to granite-gneiss (downstream). Henceforth in this paper, we refer to the reaches with sandstone bedrock as upstream reaches and the reaches with granite-gneiss bedrock as downstream reaches. Figure 2 shows the changes in channel sinuosity and bed slope along the length of Stringer Creek. These values were calculated using the measurements of channel distance (from thalweg survey) and valley distance (measured by tape). In the upstream reaches, the valley has a wider floor, the average bed slope is 5.7%, and the channel sinuosity is relatively high (maximum of 1.32). Riparian areas of upstream reaches consist mainly of grassy meadows and are mostly free of trees [*Payn et al.*, 2009]. In the downstream reaches, the channel is deeply incised into the granite-gneiss bedrock and constrained between high relief steep hill slopes, bed slopes are steeper (average slope 9.0%), and the channel sinuosity is low (1.02 near the catchment outlet). Riparian meadows are much less common in the downstream reaches and trees are found
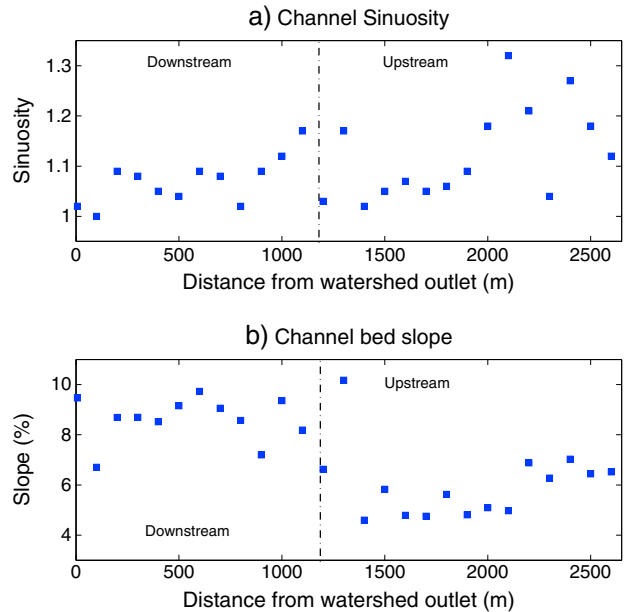
closer to the main channel. A more detailed description of the baseflow conditions, bedrock, topography, and vegetation is available in *Payn et al.* [2012].

2.2. Tracer Injection Experiments

[9] We analyzed the tracer experiments conducted in 2006 at three different flow conditions, which we henceforth refer to as high, medium, and low baseflow. Figure 3 shows the hydrograph at the watershed outlet during the spring and summer months of 2006. The high baseflow experiments were conducted from 22–24 June 2006 when the discharge at the outlet of Stringer Creek was 101 L s^{-1}. The medium baseflow experiments were conducted from 25–28 July 2006 when the estimated discharge at watershed outlet was 21 L s^{-1}. The low baseflow experiments were conducted from 26 August to 4 September, 2006 when the estimated discharge at watershed outlet was 15 L s^{-1}. The duration of individual tracer experiments ranged from 6–20 min during high baseflow, 15–45 min during medium baseflow, and 25–60 min during low baseflow. Sodium chloride (NaCl) was used as the conservative tracer.

[10] Prior to the tracer releases, 27 measurement locations were established at 100 m intervals along the main channel of Stringer Creek (see Figure 1). For each of the 27 locations, tracer was released in the main channel 10 to 30 m upstream of the measurement location. These release points were selected to ensure that there were at least three pool-riffle sequences between the injection and measurement locations, in order to mix the tracer throughout the stream [*Payn et al.*, 2009]. In each injection experiment, tracer was released instantaneously at the release point and measured at the sampling location using electrical conductivity. In each set of experiments, tracer injections were initiated at the most downstream reach (near the watershed outlet) and then progressed upstream. These tracer measurements
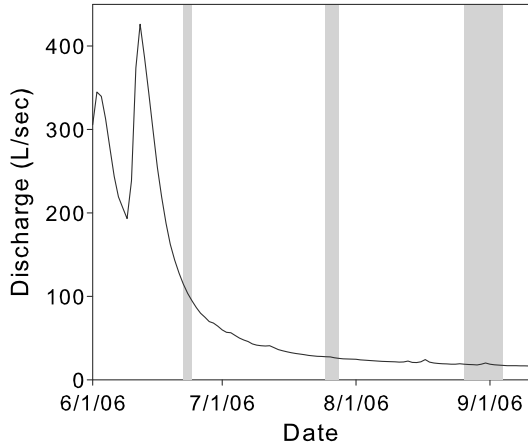
Figure 3. Hydrograph measured at the Stringer Creek watershed outlet during the summer of 2006. Gray areas represent the days (and flow conditions) when BTC measurements were obtained: 22–24 June (high baseflow), 25–28 July (medium baseflow), and 26 August to 4 September (low baseflow) (adapted from *Payn et al.* [2009]).

were also used to measure local stream discharge in each reach using the dilution gauging method, and correspond to the BTCs recorded at the upstream end of *Payn et al.* [2009] reaches. Stream velocity was calculated as a ratio of reach length to the time required to achieve peak concentration. Detailed descriptions of the experimental setup and instruments can be found in *Payn et al.* [2009].

2.3. Identification and Analysis of BTC Tails

[11] To enable a visual comparison of the 81 BTCs (27 reaches × 3 flow conditions) along the stream channel, we normalized the time and concentration axes for all BTCs. This normalization was essential since the reach lengths varied between 10 and 30 m, and different amounts of tracer were injected in each reach. Time was normalized by the time to peak concentration (t_p), whereas the tracer concentration was normalized by the peak concentration (C_p).

[12] We first identified the receding tail of each BTC and then fit this tail with a power-law equation. Several studies have suggested that the power-law tail fit provides a better characterization of solute residence times than the TSM fit [*Haggerty et al.*, 2002; *Gooseff et al.*, 2003; *Drummond et al.*, 2012]. The receding tail was identified as all the data points of a BTC that are within the t_{start} to t_{end} time period, where t_{end} is the time at which the last detectable tracer concentration of the experiment is measured and t_{start} is the time at which the receding BTC tail starts, calculated as:

$$t_{start} = t_p + \frac{t_{end} - t_p}{2}. \tag{1}$$

[13] The receding tails of all normalized BTCs were fit with the following power-law equation by minimizing the square of the residual errors:

$$C = aT^{-b}, \tag{2}$$

where C is the normalized tracer concentration, T is the normalized time, and a and b are the best-fit coefficients. Note that the normalization used here does not change the value of b, as it does not modify the shape of the BTC. The power law exponent b describes the slope of the BTC tail in log-log space, and also reflects the tail of the solute storage residence time distribution [*Metzler and Klafter*, 2000; *Berkowitz et al.*, 2006]. Shallower BTC slopes (smaller absolute values) indicate greater solute retention. When $b < 2$, the solute retention process is considered to be heavy-tailed, indicating that BTC skewness will persist indefinitely instead of decaying to regular advection-dispersion behavior [*Schumer et al.*, 2003]. We used the values of b to compare the receding tails of BTCs measured at different locations in Stringer Creek. Of the 81 measured BTCs, only the 78 BTCs whose receding tail had a statistically significant fit with equation (2) ($p < 0.010$) were considered for further analyses. We further developed regression relationships of BTC tail slopes (b) with local reach-scale properties, such as stream discharge, stream velocity, channel bed slope, and channel sinuosity. These relationships were used to identify the factors controlling the spatial and temporal variability in solute retention.
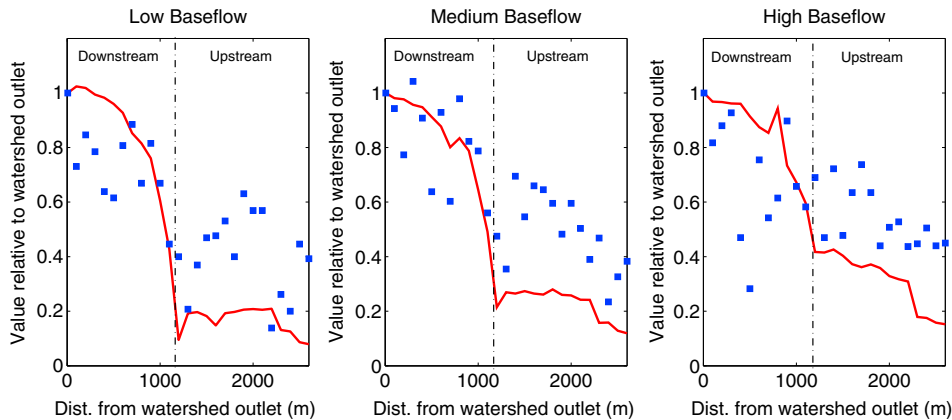

Figure 4. Stream velocity (blue squares) and discharge (solid red line) values at the 27 stream reaches along the Stringer Creek channel during the three series of tracer experiments. Values are normalized to the velocity and discharge at the watershed outlet. Black dash-dot line indicates the lithologic transition that divides the upstream and downstream reaches.

3. Results

[14] Figure 4 shows the spatial variation in stream velocity and discharge along the main channel of Stringer Creek. For all the three baseflow conditions, an abrupt increase in local stream discharge was observed below the bedrock transition that we used to distinguish upstream and downstream reaches (Figure 4). While the stream discharge persistently increased in the direction of watershed outlet, the rate of this increase was much lower in the upstream reaches than in the downstream reaches. Moreover, the rate of discharge increase in the upstream reaches was higher during high baseflow than during low and medium baseflow (Figure 4). Unlike stream discharge, the local stream velocity did not abruptly change between the upstream and downstream reaches. Stream velocity increased consistently in the downstream direction under all three flow conditions, but was subject to high local variability. Stream velocity was more variable in the downstream reaches during high baseflow, likely due to the greater complexity of the channel in downstream reaches.

[15] Figure 5 compares the normalized BTCs from five downstream reaches (7 m, 100 m, 200 m, 300 m, and 600 m upstream of watershed outlet) and five upstream reaches (1200 m, 1400 m, 1700 m, 2000 m, and 2400 m upstream of watershed outlet) under all three baseflow conditions. These BTCs were selected randomly for illustration and represent the differences in solute transport observed in the upstream and downstream reaches. During low baseflow (Figures 5e and 5f) and medium baseflow (Figures 5c and 5d), distinct differences were observed between the BTC tails in the upstream and downstream reaches. BTCs in the upstream reaches had receding tails with shallow slopes, indicating longer solute retention times. Conversely, BTCs in the downstream reaches generally had steeper receding tail slopes, indicating shorter solute retention times. However, intrastream differences were lower during high baseflow,

with no perceptible differences in the BTC tails between upstream reaches from the downstream reaches under high baseflow (Figures 5a and 5b).

[16] Figure 6 shows the tail slopes (power-law exponent b) of the 78 BTCs that were described well by equation (2), along with their 95% confidence intervals. During low baseflow, upstream reaches had much lower BTC tail slopes than downstream reaches (Figure 6a). A similar pattern occurred during medium baseflow, but with slightly greater slopes in the upstream reaches (Figure 6b). Tail slopes were even higher in upstream reaches during high baseflow, causing the tails to appear more similar between the upstream and downstream reaches under this flow condition (Figure 6c). Consistent with these observations, the coefficient of variation in BTC slopes among the 27 reaches was highest at low baseflow (CV = 0.46), and decreased for medium baseflow (CV = 0.33) and high baseflow (CV = 0.24).

[17] We analyzed the spatial variability of BTC tail slope in terms of the hydrologic (stream discharge and velocity) and geomorphic (channel slope and sinuosity) properties along Stringer Creek. Figure 7 shows the relationships of stream discharge (Q) and velocity (v) with BTC tail slope b at all 27 reaches under low, medium, and high baseflow. The relationship between Q and b is strongest at low baseflow ($R^2 = 0.48$, $p < 0.010$), and gradually weakens at medium ($R^2 = 0.39$, $p < 0.010$) and high ($R^2 = 0.20$, $p = 0.023$) baseflow. Moreover, the rate of increase in b with respect to Q is much higher for low and medium baseflow (0.165 and 0.091, respectively) than for the high baseflow (0.014). The relationship between b and v is weak compared to that of b and Q, but follows the same trend, with $R^2 = 0.25$ ($p < 0.010$) for low baseflow, 0.24 ($p < 0.010$) for medium baseflow, and 0.02 ($p = 0.500$) for high baseflow. Figure 8 shows the relationships of b with channel slope (θ) and sinuosity (S) for the three flow conditions. The relationship
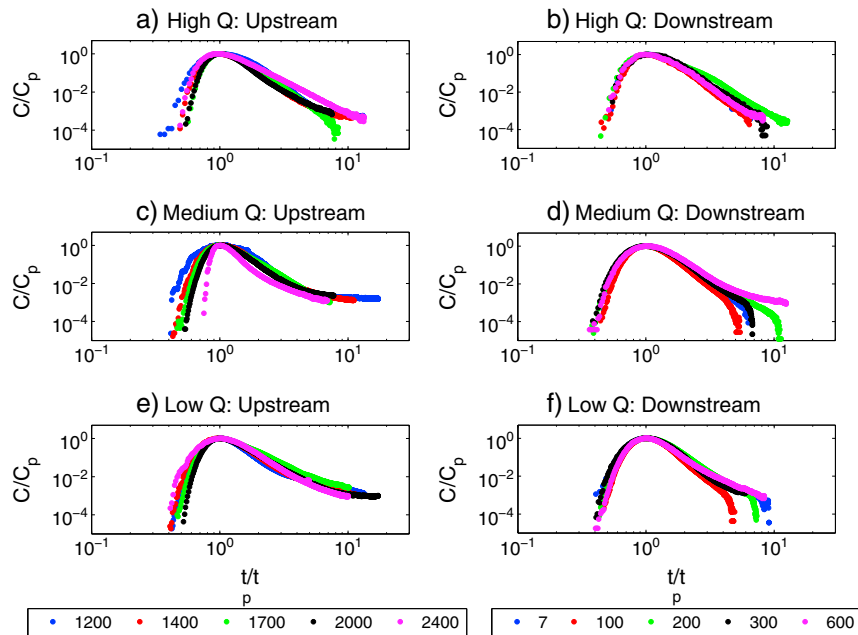

Figure 5. Normalized salt-tracer BTC concentrations at five upstream reaches (1200, 1400, 1700, 2000, and 2400 m) and five downstream reaches (7, 100, 200, 300, and 600 m) during the three baseflow conditions.
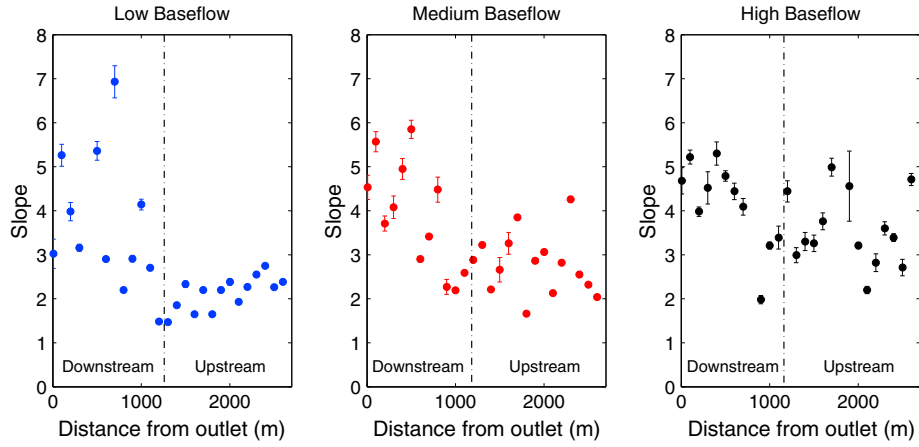
Figure 6. BTC tail slopes (b) at the 27 reaches in Stringer Creek channel during the low, medium, and high baseflow experiment (78 BTCs in total). Error bars show the 95% confidence intervals. Black dash-dot line indicates the lithologic transition that divides the upstream and downstream reaches.
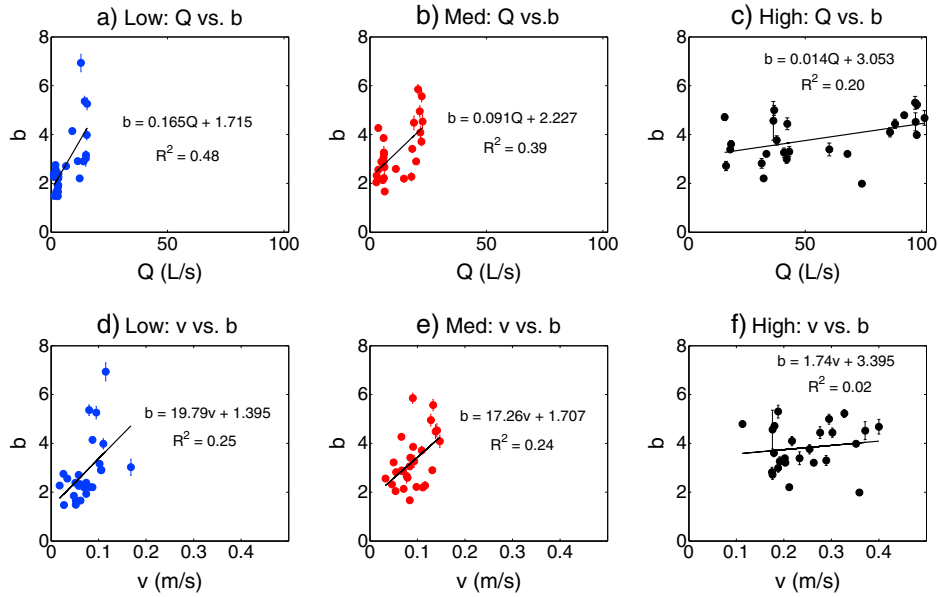

Figure 7. Relationship of BTC tail slope (b) with stream discharge (Q) and stream velocity (v) at the 27 reaches, shown separately for the low, medium, and high baseflow experiment. Error bars show the 95% confidence intervals of b.

between b and θ is strongest at low baseflow ($R^2 = 0.22$, $p = 0.014$), and weakens for medium ($R^2 = 0.13$, $p = 0.062$) and high ($R^2 = 0.03$, $p = 0.384$) baseflow. The relationship between b and S follows the opposite trend, i.e., strongest at high baseflow ($R^2 = 0.40$, $p < 0.010$), and weaker at medium ($R^2 = 0.26$, $p < 0.010$) and low ($R^2 = 0.05$, $p = 0.274$) baseflow.

[18] We also analyzed the temporal variability of BTC tail slope in terms of stream flow and velocity. Figure 9 shows the relationships of b with Q and v at all three flow conditions. The relationship between b and Q is stronger for the upstream reaches ($R^2 = 0.34$, $p < 0.010$) with a faster increase in b with respect to Q (0.036) than for the downstream reaches ($R^2 = 0.04$, $p = 0.240$) with smaller rate of increase in tail slope b (0.007). The relationship between b and v shows an even greater difference between the

upstream and downstream reaches, with a strong trend in upstream reaches ($R^2 = 0.42$, $p < 0.010$) and no significant trend in downstream reaches ($R^2 = 0.004$, $p = 0.711$).

4. Discussion

4.1. Influence of Stream Flow Conditions on Solute Retention

[19] Our results suggest that a nuanced relationship exists between solute retention and stream discharge. We found that BTC tail slopes in Stringer Creek increased rapidly with local stream discharge during low and medium baseflow, when Q varied from $1\,\mathrm{L\,s^{-1}}$ to $21\,\mathrm{L\,s^{-1}}$. This is consistent with previous studies that have found an inverse relationship between solute retention and discharge [*Harvey et al.*, 1996; *Wroblicky et al.*, 1998; *Zarnetske et al.*, 2007]. The rationale for this is straightforward since low stream discharge corresponds to low downstream flux,
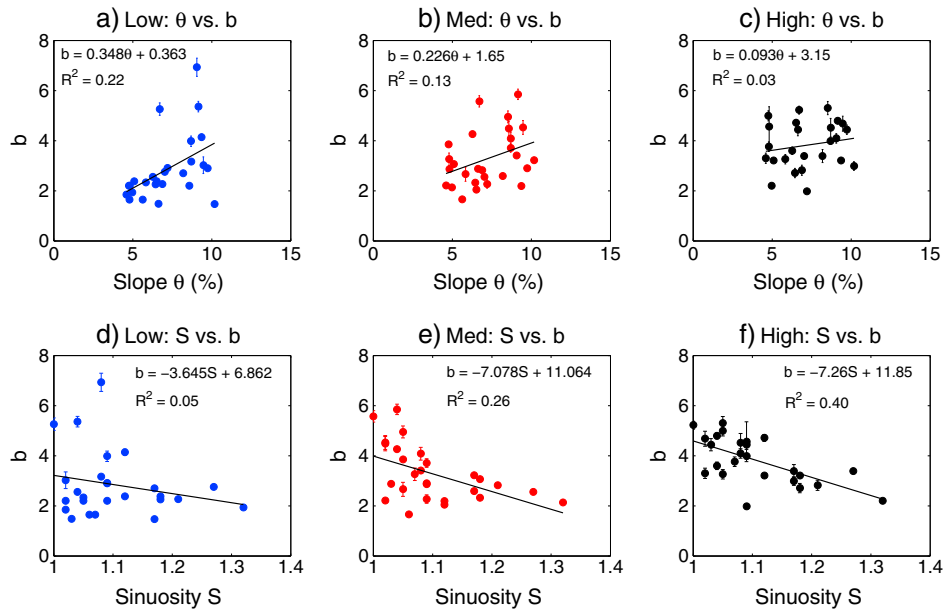
Figure 8. Relationship of BTC tail slope (b) with channel bed slope (θ) and channel sinuosity (S) at the 27 reaches, shown separately for the low, medium, and high baseflow experiment. Error bars show the 95% confidence intervals of b.
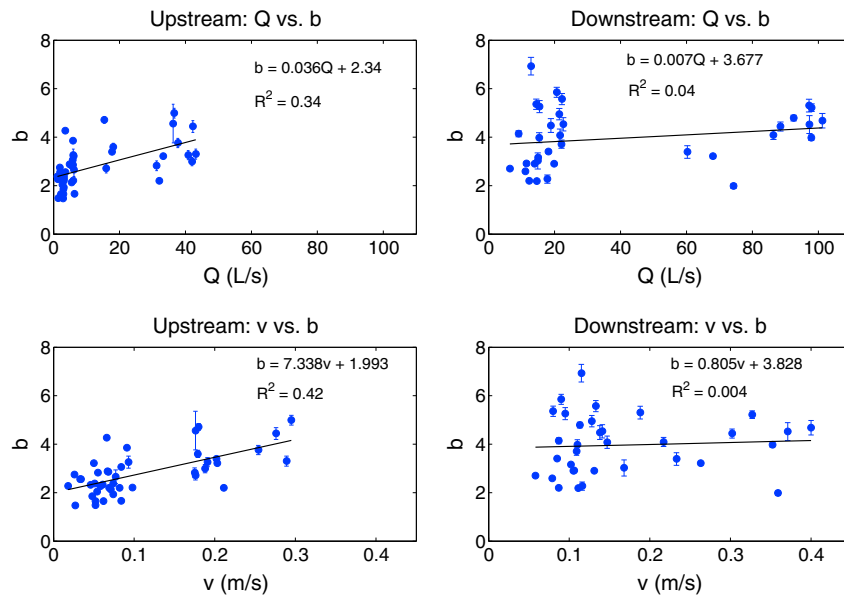

Figure 9. Relationship of BTC tail slope (b) with stream discharge (Q) and stream velocity (v) across the three baseflow experiments, shown separately for the upstream and downstream reaches. Error bars show the 95% confidence intervals of b.

which allows more time for surface-subsurface exchange of the stream water relative to downstream transport, and yields greater changes in stream water concentration for the same hyporheic exchange flux [*Bencala*, 2006]. The increase in BTC tail slope with discharge was much smaller during the period of high baseflow, when Q varied between 15 L s^{-1} and 101 L s^{-1} (Figure 7c). This suggests that the sensitivity of solute retention to local stream discharge decreases from low- to high-flow conditions. This difference in sensitivity between the low and high baseflow conditions is likely to be related to the activation of different solute storage processes, such

as development of extensive in-stream dead zones in poorly-connected side pools or backwaters at low baseflow, and transition from primarily elevation-driven hyporheic exchange at low baseflow to flow-induced hyporheic exchange at high baseflow. An important consequence of this phenomenon is that the correlation between BTC tail slope and local stream discharge in Stringer Creek decreases from low ($R^2 = 0.48$) to medium ($R^2 = 0.39$) to high ($R^2 = 0.20$) baseflow.

[20] Upstream and downstream reaches showed sharp differences in the relationships between BTC tail slope and both stream discharge and velocity (Figure 9). Tail slope

was correlated with both discharge and velocity in the upstream reaches, whereas no significant trend was observed with either flow variable in the downstream reaches. This suggests that solute retention is selectively sensitive to Q and v, i.e., it tends to be sensitive in only some types of stream reaches. While there are obvious physical differences between the upstream and downstream reaches of Stringer Creek (in terms of channel bedrock, bed slope, sinuosity, extent of riparian zone, etc.), the available data are insufficient to identify the specific mechanism that makes solute storage in Stringer Creek selectively sensitive to stream hydrology.

[21] Several potential sources of error can affect our analysis of the relationship between Q and b. Measurement of local stream discharge Q using the dilution gauging method assumes complete mass recovery of the injected tracer. However, unknown loss of the tracer mass in any reach can introduce error in the estimation of stream discharge, thereby changing the relationship between Q and b. The tracer detection limit and variability in background stream composition introduce similar uncertainty in the estimation of BTC tail slopes [*Drummond et al.*, 2012]. Incomplete mixing of the injected tracer across the stream cross section could contribute to further uncertainty. The length of each reach was selected to achieve complete mixing of the tracer before the measurement location. However, complete mixing is not guaranteed and tracer concentrations were not measured over the cross section. Incomplete tracer mixing in any reach would violate the assumptions of 1-D transport and affect the estimation of tail slope b.

4.2. Influence of Geomorphic Properties on Solute Retention

[22] Channel bed slope (θ) and channel sinuosity (S) influenced BTC tail slope in opposite ways (Figure 8). b was positively correlated with θ, but negatively correlated with S. These trends are consistent with prior observations that high channel sinuosity and the presence of meanders increases hyporheic storage [*Boano et al.*, 2007; *Cardenas*, 2009; *Stonedahl et al.*, 2010], while high channel slopes decrease storage [*Gooseff et al.*, 2006; *Hester and Doyle*, 2008]. The relationship between b and θ was strongest under low baseflow ($R^2 = 0.22$) and weakened under medium and high baseflow. This suggests that the influence of channel slope on solute retention decreases with increasing flow depth. On the other hand, the relationship between b and S was strongest under high baseflow ($R^2 = 0.40$) and became weaker as baseflow decreased. This suggests that the ability of channel sinuosity to explain spatial variations in solute retention increases as advection becomes a more dominant process.

[23] Figure 10 shows the box-and-whisker plots of tail slope b in upstream and downstream reaches across all baseflow conditions. Tail slopes were much higher in downstream reaches (median $b = 4.03$) than in upstream reaches (median $b = 2.68$). We attribute these differences to the change in channel morphology associated with the bedrock transition ~1200 m upstream of the watershed outlet. The upstream reaches are characterized by relatively high channel sinuosity, low bed slope, low stream velocity, and are underlain by sandstone bedrock. Such conditions of streamflow and morphology have been shown to increase the hyporheic retention
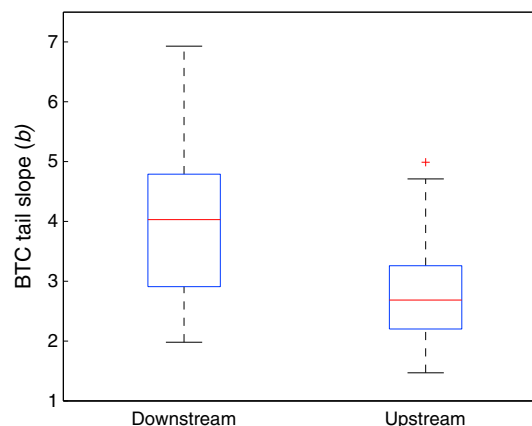

Figure 10. Box-and-whisker plots of BTC tail slope (b) across the three baseflow experiments, shown separately for the upstream and downstream reaches.

time, and thereby are expected to produce shallow BTC tails [*Harvey and Wagner*, 2000; *Boano et al.*, 2006]. Conversely, downstream of the transition point, the channel becomes straighter, slope increases, stream velocity is higher, and the bedrock material changes to granite-gneiss. Such conditions are expected to cause physical constraints on the hyporheic exchange in downstream reaches and result in steeper BTC tails. While the majority of Stringer Creek is gaining groundwater, the gains are much stronger in reaches below the bedrock transition (Figure 4). Hyporheic exchange and solute retention decrease dramatically under gaining conditions [*Cardenas and Wilson*, 2006; *Hester and Doyle*, 2008; *Stonedahl et al.*, 2012]. *Payn et al.* [2012] speculated that large gains in the downstream reaches of Stringer Creek could occur because of the intersection of the valley with larger-scale groundwater systems, which provide additional sources of water to the stream channel. Surface–groundwater interactions are often enhanced at geologic transitions, especially if the hydrologic storage and transmissivity of the downstream bedrock is lower than that of the upstream bedrock [*Wroblicky et al.*, 1998; *Sophocleous*, 2002]. However, there is no direct evidence of contributions from large-scale groundwater flow paths into Stringer Creek. Moreover, while sandstones are known to be more permeable than granites in general [*Bear*, 1972], bedrock permeability has not been measured at Stringer Creek. As a result, the underlying causes of the differences in solute storage in upstream and downstream reaches of Stringer Creek cannot be conclusively determined.

4.3. Implications for Solute Transport Along Stream Networks

[24] Understanding of the intrastream variability in solute retention becomes much more important for transport at larger scales because of the opportunity for solutes to interact with diverse storage regions that have vastly different retention timescales. This makes it especially important to (1) identify the zones within a stream network where high solute retention is likely to occur, and (2) characterize the impact of such zones on the distribution of transport timescales at the watershed scale. Our analysis of BTCs in multiple stream reaches along the Stringer Creek channel reveals the dynamic nature of solute retention in rivers. Specifically, our results suggest that solute retention

tends to become more homogeneous at higher streamflow conditions. At the scale of individual stream reaches, solute retention can be highly sensitive to hydrologic fluctuations. However, this sensitivity appears to be influenced by local geomorphic conditions (Figure 9).

[25] The intrastream variability in solute transport dynamics that we observed in Stringer Creek has not been characterized previously, as most prior studies have focused on solute transport behavior over timescales of hours to days in relatively homogeneous stream reaches. Solute transport is expected to generally become more homogeneous through watersheds under higher flows that obscure local geomorphic complexity. This effect can partly be seen in the relationship between relative roughness (bed roughness relative to flow depth) and friction factor. Friction factors are positively correlated with solute storage parameters [*Harvey and Wagner*, 2000], indicating that storage should decrease with increasing submergence of streambed roughness. More basic analysis of flow-boundary interactions also indicates that hyporheic exchange will decrease with increasing submergence of bedforms under the same average stream velocity [*Elliott and Brooks*, 1997]. Surface-groundwater interactions are driven by multiple mechanisms, some of which increase with stream flow, while others are relatively insensitive to stream flow. Hyporheic exchange induced by flow-boundary interactions increase strongly with stream velocity (and shear velocity), while exchange associated with elevation head gradients (e.g., across meanders or between multiple channels in braided streams) and large-scale surface-groundwater interactions only vary weakly with stream velocity [*Packman and Bencala*, 2000; *Cardenas*, 2008; *O'Connor and Harvey*, 2008; *Grant and Marusic*, 2011]. The relative importance of exchange induced by flow-boundary interactions is expected to increase with increasing discharge, but these effects are counteracted by the increasing downstream flux and the lower ratio of bed surface area to stream volume at higher stream discharge. The results presented here suggest that there are changes in the balance between these different mechanisms both spatially within Stringer Creek and temporally as baseflow conditions change. The interplay of these mechanisms should be investigated in other types of rivers to better characterize the interaction of discharge, channel morphology, and solute transport.

5. Summary and Conclusion

[26] We analyzed multiple salt-tracer BTCs measured in 27 small reaches and under three different baseflow conditions along the stream channel of Stringer Creek, which drains a $5.5 \, km^2$ watershed within the Tenderfoot Creek Experimental Forest, Montana. Results showed that the BTCs in upstream reaches had receding tails with small slopes, indicating higher solute retention. Conversely, BTCs in the downstream reaches had receding tails with higher slopes, indicating lower solute retention relative to the upstream reaches. Intrastream differences in BTC tails, apparently driven by structural differences between upstream and downstream reaches, were distinctly observable only when the overall streamflow conditions were sufficiently low. Spatial variability of BTC tail slopes was lowest during high baseflow and increased during medium and low baseflow. This variability was best explained by the spatial

variations of local stream discharge during low baseflow ($R^2 = 0.48$), and channel sinuosity during high baseflow ($R^2 = 0.40$). The relationships between BTC tail slope and channel geomorphic properties (slope and sinuosity) were sensitive to changes in stream flow. This suggests that the influence of geomorphic properties on solute retention behavior is regulated by hydrologic conditions. BTC tail slopes were sensitive to hydrologic properties (discharge and velocity) at upstream reaches but not in downstream reaches, most likely due to the differences in channel morphology. While we expect the findings from this study to be applicable to a wide variety of streams, there is a dearth of detailed data on solute retention in most geographic settings. We recommend investigation of the spatial and temporal patterns of solute transport in all major classes of watersheds.

References

Alexander, R., J. Böhlke, E. Boyer, M. David, J. Harvey, P. Mulholland, S. Seitzinger, C. Tobias, C. Tonitto, and W. Wollheim (2009), Dynamic modeling of nitrogen losses in river networks unravels the coupled effects of hydrological and biogeochemical processes, *Biogeochemistry*, *93*(1), 91–116, doi:10.1007/s10533-008-9274-8.

Battin, T. J., L. A. Kaplan, S. Findlay, C. S. Hopkinson, E. Marti, A. I. Packman, J. D. Newbold, and F. Sabater (2008), Biophysical controls on organic carbon fluxes in fluvial networks, *Nat. Geosci.*, *1*(2), 95–100, doi:10.1038/ngeo101.

Bear, J. (1972), Dynamics of Fluids in Porous Media, p. 764, Elsevier, New York.

Bencala, K. E. (2006), Hyporheic exchange flows, in Encyclopedia of Hydrological Sciences, edited by, John Wiley and Sons, New York.

Bencala, K. E., and R. A. Walters (1983), Simulation of solute transport in a mountain pool-and-riffle stream: A transient storage model, *Water Resour. Res.*, *19*(3), 718–724, doi:10.1029/WR019i003p00718.

Berkowitz, B., A. Cortis, M. Dentz, and H. Scher (2006), Modeling non-Fickian transport in geological formations as a continuous time random walk, *Rev. Geophys.*, *44*(2), RG2003, doi:10.1029/2005RG000178.

Boano, F., C. Camporeale, R. Revelli, and L. Ridolfi (2006), Sinuosity-driven hyporheic exchange in meandering rivers, *Geophys. Res. Lett.*, *33*, L18406, doi:10.1029/2006GL027630.

Boano, F., A. I. Packman, A. Cortis, R. Revelli, and L. Ridolfi (2007), A continuous time random walk approach to the stream transport of solutes, *Water Resour. Res.*, *43*, W10425, doi:10.1029/2007WR006062.

Bockelmann, B. N., E. K. Fenrich, B. Lin, and R. A. Falconer (2004), Development of an ecohydraulics model for stream and river restoration, *Ecol. Eng.*, *22*(4–5), 227–235, doi:10.1016/j.ecoleng.2004.04.003.

Boult, S., D. N. Collins, K. N. White, and C. D. Curtis (1994), Metal transport in a stream polluted by acid mine drainage—The Afon Goch, Anglesey, UK, *Environ. Pollut.*, *84*(3), 279–284, doi:10.1016/0269-7491(94)90139-2.

Bukaveckas, P. A. (2007), Effects of channel restoration on water velocity, transient storage, and nutrient uptake in a channelized stream, *Environ. Sci. Technol.*, *41*(5), 1570–1576, doi:10.1021/es061618x.

Cardenas, M. B. (2008), Surface water-groundwater interface geomorphology leads to scaling of residence times, *Geophys. Res. Lett.*, *35*, L08402, doi:10.1029/2008GL033753.

Cardenas, M. B. (2009), A model for lateral hyporheic flow based on valley slope and channel sinuosity, *Water Resour. Res.*, *45*, W01501, doi:10.1029/2008WR007442.

Cardenas, M. B., J. L. Wilson, and V. A. Zlotnik (2004), Impact of heterogeneity, bed forms, and stream curvature on subchannel hyporheic exchange, *Water Resour. Res.*, *40*, W08307, doi:10.1029/2004WR003008.

Cardenas, M. B., and J. L. Wilson (2006), The influence of ambient groundwater discharge on exchange zones induced by current–bedform interactions, *J. Hydrol.*, *331*(1–2), 103–109, doi:10.1016/j.jhydrol.2006.05.012.

Choi, J., J. W. Harvey, and M. H. Conklin (2000), Characterizing multiple timescales of stream and storage zone interaction that affect solute fate and transport in streams, *Water Resour. Res.*, *36*, 1511–1518, doi:10.1029/2000WR900051.

D'Angelo, D. J., J. R. Webster, S. V. Gregory, and J. L. Meyer (1993), Transient storage in appalachian and cascade mountain streams as related to hydraulic characteristics, *J. N. A. Benthol. Soc.*, *12*(3), 223–235.

Da Silva, E. F., E. C. Fonseca, J. X. Matos, C. Patinha, P. Reis, and J. M. Santos Oliveira (2005), The effect of unconfined mine tailings on the geochemistry of soils, sediments and surface waters of the lousal area (Iberian Pyrite Belt, Southern Portugal), *Land Degrad. Dev.*, *16*(2), 213–228, doi:10.1002/ldr.659.

Doyle, M. W., and R. L. Fuller (2011), Quantitatively evaluating restoration scenarios for rivers with recreational flow releases, in Stream Restoration in Dynamic Fluvial Systems: Scientific Approaches, Analyses, and Tools, Geophys. Monogr. Ser., vol. *194*, edited by A. Simon et al., 544 pp., AGU, Washington, D. C., doi:10.1029/GM194.

Drummond, J. D., T. P. Covino, A. F. Aubeneau, D. Leong, S. Patil, R. Schumer, and A. I. Packman (2012), Effects of solute breakthrough curve tail truncation on residence time estimates: A synthesis of solute tracer injection studies, *J. Geophys. Res.*, *117*, G00N08, doi:10.1029/2012JG002019.

Elliott, A. H., and N. H. Brooks (1997), Transfer of nonsorbing solutes to a streambed with bed forms: Theory, *Water Resour. Res.*, *33*(1), 123–136, doi:10.1029/96WR02784.

Gooseff, M. N., S. M. Wondzell, R. Haggerty, and J. Anderson (2003), Comparing transient storage modeling and residence time distribution (RTD) analysis in geomorphically varied reaches in the Lookout Creek basin, Oregon, USA, *Adv. Water Resour.*, *26*(9), 925–937, doi:10.1016/s0309-1708(03)00105-2.

Gooseff, M. N., J. K. Anderson, S. M. Wondzell, J. LaNier, and R. Haggerty (2006), A modelling study of hyporheic exchange pattern and the sequence, size, and spacing of stream bedforms in mountain stream networks, Oregon, USA, *Hydrol. Proc.*, *20*(11), 2443–2457, doi:10.1002/hyp.6349.

Gooseff, M. N., R. O. Hall, Jr., and J. L. Tank (2007), Relating transient storage to channel complexity in streams of varying land use in Jackson Hole, Wyoming, *Water Resour. Res.*, *43*, W01417, doi:10.1029/2005WR004626.

Gooseff, M. N., K. E. Bencala, and S. M. Wondzell (2008), Solute transport along stream and river networks, in River Confluences, Tributaries and the Fluvial Network, edited, pp. 395–417, John Wiley and Sons, New York.

Grant, S. B., and I. Marusic (2011), Crossing turbulent boundaries: Interfacial flux in environmental flows, *Environ. Sci. Technol.*, *45*(17), 7107–7113, doi:10.1021/es201778s.

Haggerty, R., S. M. Wondzell, and M. A. Johnson (2002), Power-law residence time distribution in the hyporheic zone of a 2nd-order mountain stream, *Geophys. Res. Lett.*, *29*(13), 1640, doi:10.1029/2002GL014743.

Harvey, J. W., and B. J. Wagner (2000), Quantifying hydrologic interactions between streams and their subsurface hyporheic zones, in Streams and ground waters, edited, Academic Press, San Diego, Calif.

Harvey, J. W., B. J. Wagner, and K. E. Bencala (1996), Evaluating the reliability of the stream tracer approach to characterize stream-subsurface water exchange, *Water Resour. Res.*, *32*(8), 2441–2451, doi:10.1029/96WR01268.

Hester, E. T., and M. W. Doyle (2008), In-stream geomorphic structures as drivers of hyporheic exchange, *Water Resour. Res.*, *44*, W03417, doi:10.1029/2006WR005810.

Hester, E. T., and M. N. Gooseff (2010), Moving beyond the banks: Hyporheic restoration is fundamental to restoring ecological services and functions of streams, *Environ. Sci. Technol.*, *44*(5), 1521–1525, doi:10.1021/es902988n.

Hussein, M., and F. W. Schwartz (2003), Modeling of flow and contaminant transport in coupled stream–aquifer systems, *J. Contam. Hydrol.*, *65*(1–2), 41–64, doi:10.1016/s0169-7722(02)00229-2.

Jones, J. B., and P. J. Mulholland (2000), Streams and GROUND WATERS, Academic Press, San Diego, Calif.

Karwan, D. L., and J. E. Saiers (2009), Influences of seasonal flow regime on the fate and transport of fine particles and a dissolved solute in a New England stream, *Water Resour. Res.*, *45*, W11423, doi:10.1029/2009WR008077.

Metzler, R., and J. Klafter (2000), The random walk's guide to anomalous diffusion: A fractional dynamics approach, *Phys. Rep.*, *339*(1), 1–77, doi:10.1016/s0370-1573(00)00070-3.

O'Connor, B. L., and J. W. Harvey (2008), Scaling hyporheic exchange and its influence on biogeochemical reactions in aquatic ecosystems, *Water Resour. Res.*, *44*, W12423, doi:10.1029/2008WR007160.

O'Connor, B. L., M. Hondzo, and J. W. Harvey (2010), Predictive modeling of transient storage and nutrient uptake: Implications for stream restoration, *J. Hydraul. Eng.*, *136*(12), 1018–1032, doi:10.1061/(ASCE)HY.1943-7900.0000180.

Packman, A. I., and K. E. Bencala (2000), Modeling surface-subsurface hydrological interactions, in Streams and Ground Waters, edited, pp. 45–80, Academic Press, San Diego, Calif.

Packman, A. I., and J. S. MacKay (2003), Interplay of stream-subsurface exchange, clay particle deposition, and streambed evolution, *Water Resour. Res.*, *39*(4), 1097, doi:10.1029/2002WR001432.

Packman, A. I., N. H. Brooks, and J. J. Morgan (2000a), A physicochemical model for colloid exchange between a stream and a sand streambed with bed forms, *Water Resour. Res.*, *36*(8), 2351–2361, doi:10.1029/2000WR900059.

Packman, A. I., N. H. Brooks, and J. J. Morgan (2000b), Kaolinite exchange between a stream and streambed: Laboratory experiments and validation of a colloid transport model, *Water Resour. Res.*, *36*(8), 2363–2372, doi:10.1029/2000WR900058.

Payn, R. A., M. N. Gooseff, B. L. McGlynn, K. E. Bencala, and S. M. Wondzell (2009), Channel water balance and exchange with subsurface flow along a mountain headwater stream in Montana, United States, *Water Resour. Res.*, *45*, W11427, doi:10.1029/2008WR007644.

Payn, R. A., M. N. Gooseff, B. L. McGlynn, K. E. Bencala, and S. M. Wondzell (2012), Exploring changes in the spatial distribution of stream baseflow generation during a seasonal recession, *Water Resour. Res.*, *48*, W04519, doi:10.1029/2011WR011552.

Runkel, R. L. (1998), One-dimensional transport with inflow and storage (OTIS): A solute transport model for streams and rivers, *U.S. Geol. Surv. Water Resour. Invest. Rep. 98-4018*, 73 pp.

Salehin, M., A. I. Packman, and A. Wörman (2003), Comparison of transient storage in vegetated and unvegetated reaches of a small agricultural stream in Sweden: Seasonal variation and anthropogenic manipulation, *Adv. Water Resour.*, *26*(9), 951–964, doi:10.1016/s0309-1708(03)00084-8.

Schumer, R., D. A. Benson, M. M. Meerschaert, and B. Baeumer (2003), Fractal mobile/immobile solute transport, *Water Resour. Res.*, *39*(10), 1296, doi:10.1029/2003WR002141.

Schumer, R., M. M. Meerschaert, and B. Baeumer (2009), Fractional advection-dispersion equations for modeling transport at the Earth surface, *J. Geophys. Res.*, *114*, F00A07, doi:10.1029/2008JF001246.

Sophocleous, M. (2002), Interactions between groundwater and surface water: the state of the science, *Hydrogeol. J.*, *10*(1), 52–67, doi:10.1007/s10040-001-0170-8.

Stonedahl, S. H., J. W. Harvey, A. Wörman, M. Salehin, and A. I. Packman (2010), A multiscale model for integrating hyporheic exchange from ripples to meanders, *Water Resour. Res.*, *46*, W12539, doi:10.1029/2009WR008865.

Stonedahl, S. H., J. W. Harvey, J. Detty, A. Aubeneau, and A. I. Packman (2012), Physical controls and predictability of stream hyporheic flow evaluated with a multiscale model, *Water Resour. Res.*, *48*, W10513, doi:10.1029/2011WR011582.

Szeftel, P., R. D. Moore, and M. Weiler (2011), Influence of distributed flow losses and gains on the estimation of transient storage parameters from stream tracer experiments, *J. Hydrol.*, *396*(3–4), 277–291, doi:10.1016/j.jhydrol.2010.11.018.

Tonina, D., and J. M. Buffington (2009), Hyporheic exchange in Mountain Rivers I: Mechanics and environmental effects, *Geogr. Compass*, *3*(3), 1063–1086, doi:10.1111/j.1749-8198.2009.00226.x.

von Schiller, D., E. Martí, J. Riera, M. Ribot, A. Argerich, P. Fonollà, and F. Sabater (2008), Inter-annual, annual, and seasonal variation of P and N retention in a perennial and an intermittent stream, *Ecosystems*, *11*(5), 670–687, doi:10.1007/s10021-008-9150-3.

Wondzell, S. M. (2006), Effect of morphology and discharge on hyporheic exchange flows in two small streams in the Cascade Mountains of Oregon, USA, *Hydrol. Proc.*, *20*(2), 267–287, doi:10.1002/hyp.5902.

Wörman, A., A. I. Packman, H. Johansson, and K. Jonsson (2002), Effect of flow-induced exchange in hyporheic zones on longitudinal transport of solutes in streams and rivers, *Water Resour. Res.*, *38*(1), 1001, doi:10.1029/2001WR000769.

Wroblicky, G. J., M. E. Campana, H. M. Valett, and C. N. Dahm (1998), Seasonal variation in surface-subsurface water exchange and lateral hyporheic area of two stream-aquifer systems, *Water Resour. Res.*, *34*(3), 317–328, doi:10.1029/97WR03285.

Zarnetske, J. P., M. N. Gooseff, T. R. Brosten, J. H. Bradford, J. P. McNamara, and W. B. Bowden (2007), Transient storage as a function of geomorphology, discharge, and permafrost active layer conditions in Arctic tundra streams, *Water Resour. Res.*, *43*, W07410, doi:10.1029/2005WR004816.